Proceedings of the ASME 2017 Conference on Smart Materials, Adaptive Structures and Intelligent Systems
SMASIS 2017
September 18-20, 2017, Snowbird, USA

# SMASIS2017-3917

# NETWORK THEORETIC APPROACH TO ATOMISTIC MATERIAL MODELING USING SPECTRAL SPARSIFICATION

Peter C. Woerner, Aditya G. Nair, Kunhiko Taira, William S. Oates\*
Department of Mechanical Engineering
Florida A&M University & Florida State University
Tallahassee, Florida 32310
woates@fsu.edu

## **ABSTRACT**

Network theory is used to formulate an atomistic material network. Spectral sparsification is applied to the network as a method for approximating the interatomic forces. Local molecular forces and the total force balance is quantified when the internal forces are approximated. In particular, we compare spectral sparsification to conventional thresholding (radial cut-off distance) of molecular forces for a Lennard–Jones potential and a Coulomb potential. The spectral sparsification for the Lennard–Jones potential yields comparable results while spectral sparsification of the Coulomb potential outperforms the thresholding approach. The results show promising opportunities which may accelerate molecular simulations containing long-range electrical interactions which are relevant to many multifunctional materials.

#### INTRODUCTION

Molecular dynamics (MD) is a frequently used numerical tool for simulating the properties of fluids, solids, and molecules [1,2]. Atoms are treated as point masses and numerical integration of Newton's equations yields their trajectories over time. A variety of useful micro- and macroscopic information can be extracted from ensembles of simulated atoms including, but not limited to, mechanical [1,3,4] and thermal properties [5–7].

Large scale MD simulations containing millions of atoms are computationally expensive [8]. These computations require

many time steps to obtain statistically meaningful thermodynamic relations [1,2]. The time step is constrainted by the highest frequency of atomic vibrations: typically on the order of femtoseconds. As such, nanosecond simulations will necessitate millions of time steps [1].

Extensive effort on improving the computational speed of MD simulations have focused on massively parallel implementation of MD simulations [1]. Both specialized hardware and novel algorithms have been developed [1,9–12]. However, many algorithms suffer accuracy limitations when the forces are longrange. For short-range potentials such as Lennard–Jones, these algorithms typically use a cutoff distance above which interactions are neglected (referred to as thresholding). This is often sufficient for short-range forces from isotropic potentials; however, minimizing the error becomes uncertain when using long-range forces or angular dependent forces. These long-range forces are particularly pervasive in a variety of smart materials, including ferroelectric single crystals, electrostrictive polymers, and magnetostrictive materials.

Here, we examine the structure of the molecular interactions using network theory and utilize the network-based tools to develop computationally inexpensive representations of the molecular interactions. Network theory has long been used to describe various complex systems including airplane scheduling, social interactions and electric grids [13]. It has also been used in engineering systems such as fluid dynamics [14–17], chemical networks [18] and dynamics of granular matter [19,20], but minimal research has investigated its application to solid mechanics. A

<sup>\*</sup>Address all correspondence to this author.

network consists of a series of points (nodes) and their pairwise interactions (edges) [13]. The tools of network theory describe the bulk structure based on the underlying interactions that govern the system dynamics [13].

Given a network-based representation of a system, one can consider determining a sparse network representation to distill the network to its core features or to extract its important structure and correlation with material properties. One technique is known as the spectral sparsification method, which quantifies the spectra of the graph while finding its sparse representation [21, 22]. The goal of the current work is to determine whether spectral sparsification is a viable algorithm for speeding up computation and reducing errors in MD simulations.

The application of spectral sparsification to molecular dynamics is described using examples based upon a simple Lennard–Jones potential and a Coulombic potential. It is shown that spectral sparsification can conserve system properties but reorganizes atomic interaction force distribution in order to achieve a sparse model. After first introducing molecular dynamics and network theory, the atomistic model is numerically implemented and errors using thresholding versus sparsification are quantified. Finally, we conclude with suggestions for future work and potential applications.

#### **Molecular Dynamics**

Molecular dynamics models consist of a large collection of atoms as point masses and calculates atomic trajectories  $(\mathbf{x})$  via Newton's law

$$\sum \mathbf{F} = m\mathbf{a},\tag{1}$$

where **F** are the local forces within the solid, m is the mass and  $\mathbf{a} = \ddot{\mathbf{x}}$  is the acceleration [1,2]. The force is typically calculated from the negative gradient of a potential

$$\mathbf{F} = -\nabla U,\tag{2}$$

where U is the potential energy. The most simple potentials are pair functions based on the distance between two atoms

$$U_{ij} = U(r_{ij}), \tag{3}$$

where  $r_{ij}$  is the interatomic distance between atoms i and j [2]. The absolute position of atom i is denoted by  $\mathbf{r}_i$ .

The Lennard-Jones potential is given by

$$U_{ij}^{LJ} = \varepsilon_0 \left[ \left( \frac{\sigma}{r_{ij}} \right)^{12} - \left( \frac{\sigma}{r_{ij}} \right)^6 \right], \tag{4}$$

where  $\varepsilon_0$  is the energy well and  $\sigma$  is the zero potential distance. The potential  $U_{ij}$  defines the energy between two specific atoms and the total energy is calculated by summing all pairwise potentials.

The Coulomb potential is given by

$$U_{ij}^{C} = \frac{kq_{i}q_{j}}{\varepsilon_{m}r_{ii}},\tag{5}$$

which describes interactions between charges where k is Coulomb's constant,  $\varepsilon_m$  is the medium permittivity, and  $q_i$  and  $q_j$  are the charges of the two atoms [23].

# **Network Theory**

We first define relations associated with nodes and edges that are utilized in network theory. This is followed by its application in describing and sparsifying atomistic interactions and sparsification methods.

**Formulation** A network is a collection of vertices which are connected by edges [13]. A graph G is an ordered set G = (V, E, w(E)) consisting of the nonempty set  $V = \{v_1, v_2, ..., v_N\}$  of vertices or nodes, the set E of edges describing connected pairs of vertices, and the function w(E) which assigns each edge a numerical weight [13]. If the weights are all set to zero or one, the graph is called unweighted. In contrast, if the weights take positive real numbers, the graph is said to be weighted. A graph is directed if  $w_{ij} \neq w_{ji}$ . Otherwise, it is undirected where  $w_{ij} = w_{ji}$ . A complete graph is a graph in which all pairs of vertices have an edge between them.

Network connections are frequently algebraically described by the adjacency matrix  $A \in \Re^{N \times N}$ 

$$A_{ij} = \begin{cases} w_{ij} & \text{if } (i,j) \in E \\ 0 & \text{otherwise.} \end{cases}$$
 (6)

The adjacency matrix of an undirected graph is symmetric.

The second matrix associated with graphs is the graph Laplacian  $L \in \Re^{N \times N}$ 

$$L_{ij} = \begin{cases} k_i & \text{if } i = j \\ -w_{ij} & \text{if } (i, j) \in E \\ 0 & \text{otherwise,} \end{cases}$$
 (7)

where  $k_i = \sum_j A_{ij}$  is the degree of vertex *i*. The graph Laplacian is considered analogous to the continuous Laplacian operator  $(-\nabla^2)$ . The graph Laplacian and the adjacency matrices form the basis of graph-theoretic framework and most evaluations of the structure of a graph are generally assessed by examining these two matrices [13].

**Application to Atomistic Interactions** With respect to atomistic networks, there are different physical properties that may be projected onto the network. In this work, we take the individual atoms as the nodes. The edge weights could be a function of distance, the pairwise potential energy, or the pairwise force. Since the force is a vector quantity, the magnitude of the force is considered for the scalar edge weights. The atomistic network edge is therefore given by the magnitude of the force between two atoms separated by  $r_{ij}$ 

$$w_{ij} = |F_{ij}|. (8)$$

While there are many different metrics for which the network structure can be used [13], we consider the degree and degree distribution. The degree is defined on each node by

$$k_i = \sum_j A_{ij}. (9)$$

The degree distribution can then be represented by a histogram to illustrate changes in properties of the graph as a function of the internal molecular forces. The nodal degree is one of the most prominent metrics used in network theory [13]. It is particularly important to the current application because describes the total force on each particle.

**Atomistic Network Sparsification** Sparsification involves approximating a network, G, with a sparse network  $G_s$  [21]. Sparsification is based on the idea of network similarity. A number of different methods have been described based on different graph topology metrics [24,25]. Spectral sparsification has been identified as being advantageous for studying dynamics on networks [14].

For spectral sparsification, an approximation order denoted by  $\varepsilon$  is chosen to have the sparse graph satisfy

$$(1 - \varepsilon)v^T L v \le v^T L_s v \le (1 + \varepsilon)v^T L v \tag{10}$$

for all  $v \in \mathbb{R}^N$  where L is the graph Laplacian,  $L_s$  is the sparsified graph Laplacian [21]. If  $\varepsilon = 0$  there is no sparsification

of the network while  $\varepsilon = 1$  gives the maximum amount of sparsification allowed by the algorithm. The algorithm for spectral sparsification is described by the following four steps [14,21]:

1. Calculate the Moore–Penrose pseudoinverse of the Laplacian matrix,  $L^+$ , and use it to calculate the effective resistance by the formula

$$\hat{R}_{ij} = (p_i - q_j)^T L^+(p_i - q_j), \tag{11}$$

where p and q are the vector representation of the nodes. For example, the node labeled one will have  $p_1 = (1,0,\ldots,0) = q_1$ .

- 2. Select an edge at random with the probability of keeping the edge proportional to its effective resistance,  $\hat{R}_{ij}$ . This probability is,  $p_{ij} = \hat{R}_{ij}/\sum_{ij}\hat{R}_{ij}$ .
- 3. Add the selected edge to the sparse graph  $G_S$  with weight  $\hat{w}_{ij} = w_{ij}/qp_{ij}$ , where q is the number of samples  $q = 8N\log_2(N)/\varepsilon^2$ .
- 4. Sample *q* times and sum up weights that are selected more than once. Any edges that are not selected are removed.

Spectral sparsification provides a novel way to potentially speed up and reduce error in MD simulations especially when dealing with long-range forces. The preceding algorithm is implemented and tested in this paper using a two-dimensional square model with a circular hole. In particular, we demonstrate that spectral sparsification accurately conserves the total force in the presence of long-range forces relative to conventional molecular dynamic threshold approximations. Multiple other methods exist, e.g fast multipole method [26–30]; however, the present analysis serves as a simple alternative to facilitate computational speed-up without introducing large errors.

### Implementation and Results

The present analysis looks at both the Lennard–Jones potential and the Coulomb potential by considering a two-dimensional test problem consisting of a crystalline material with a circular hole (see Figure 1). We compare example graphs generated without sparsification, with thresholding at the most frequently used radial cutoff length, and spectral sparsification with varying edge densities as governed by  $\varepsilon$ , introduced in (10).

We define near equilibrium position, as the atom positions located in the minimum energy position for a perfect, infinitely large, zero temperature crystal. This means near equilibrium does not account for surface relaxation on the boundary of our finite crystal or relaxation around the hole. For a test problem, we use a square with a hole in the middle as shown in Figure 1. The test configuration has a width and height of 30 unit cells with a hole in the center with a radius of 5 unit cells. Note that for the Lennard–Jones potential, the atoms have no charge.

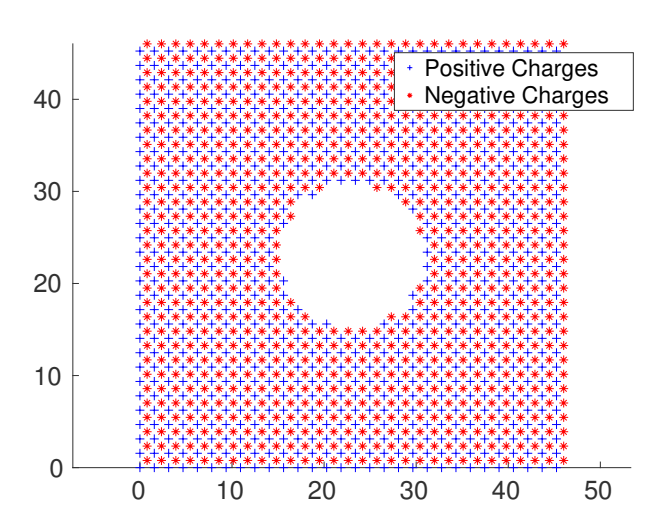


**FIGURE 1.** CHARGE AND ATOM ARRANGEMENT FOR TESTING SPARSIFICATION OF THE COULOMB AND LENNARD JONES POTENTIALS.

Figures 2 and 3 show images of the original graph, thresholding at  $r_{cut}=2.5\sigma$  and an example graph from spectral sparsification with  $\varepsilon=1$ . Figures 2 and 3 shows these graphs based on the Lennard Jones potential and the Coulomb potential, respectively. Note that both spectral sparsification and thresholding remove the interactions across the hole. For Lennard-Jones, the spectrally sparsified graph has fewer edges than thresholding. For the Coulombic potential, thresholding generates a more sparse graph, however it does so by removing significant longranged forces.

We examine the net normalized forces versus the fraction of edges removed in Figures 4 and 5. The normalized net force  $\tilde{F}$  is defined by

$$\tilde{F} = \frac{\sum_{ij} A_{ij}^s}{\sum_{ij} A_{ij}},\tag{12}$$

where  $A_{ij}^s$  and  $A_{ij}$  are the adjacency matrices of the sparsified and original graphs, respectively. This is the sum of the magnitude of all the force interactions in the network. To quantify the amount of edge sparsification, the fraction of remaining edges  $F_e$  is evaluated with

$$F_e = 1 - \frac{N_e^s}{N_e^o},\tag{13}$$

where  $N_e^s$  is the number of nonzero edges in the sparsified

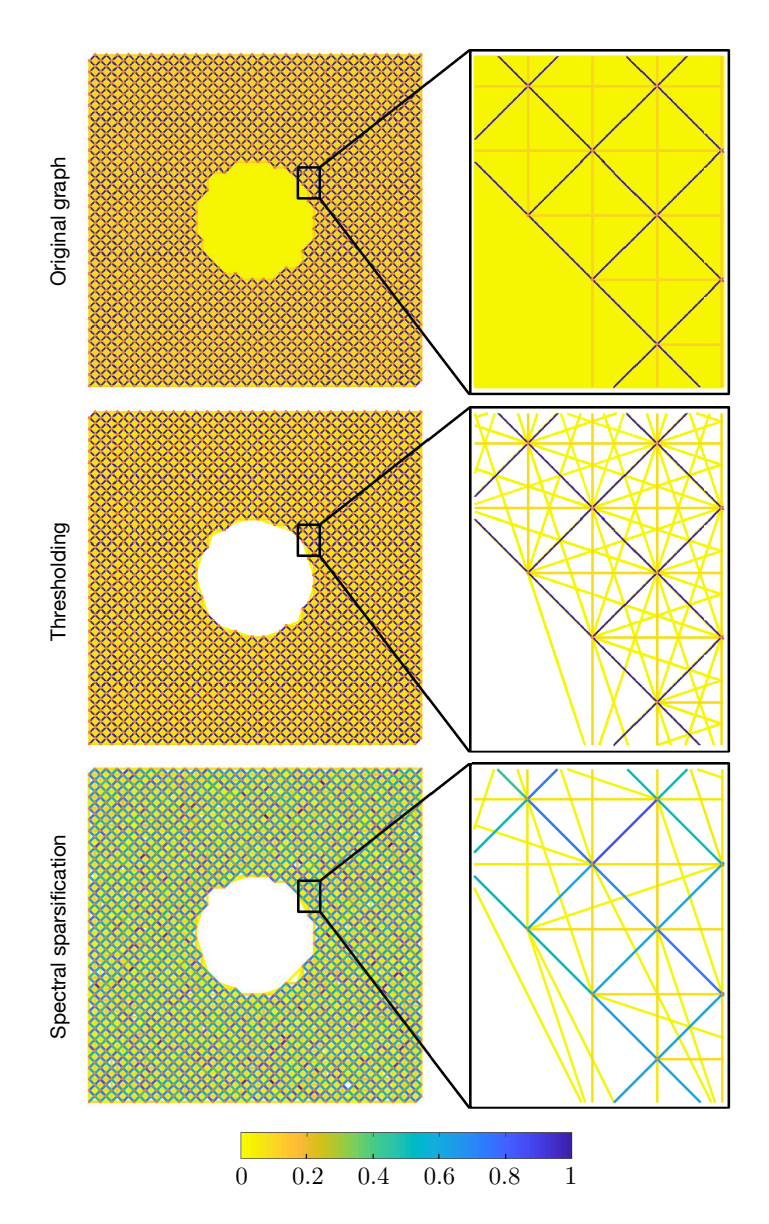


**FIGURE 2**. LENNARD–JONES FORCE GRAPHS WITH SPAR-SIFICATION BY THRESHOLDING AND SPECTRAL SPARSIFI-CATION. THE COLOR REPRESENTS THE NORMALIZED EDGE WEIGHT.

graph and  $N_e^o$  is the number of nonzero edges in the original graph. Spectral sparsification shows superior conservation of total forces; particularly for the case of the Coulomb potential.

Figures 6 and 7 show the average normalized error of the degree at each node. In terms of molecular mechanics, this error describes the change in the magnitude of forces on each atom.

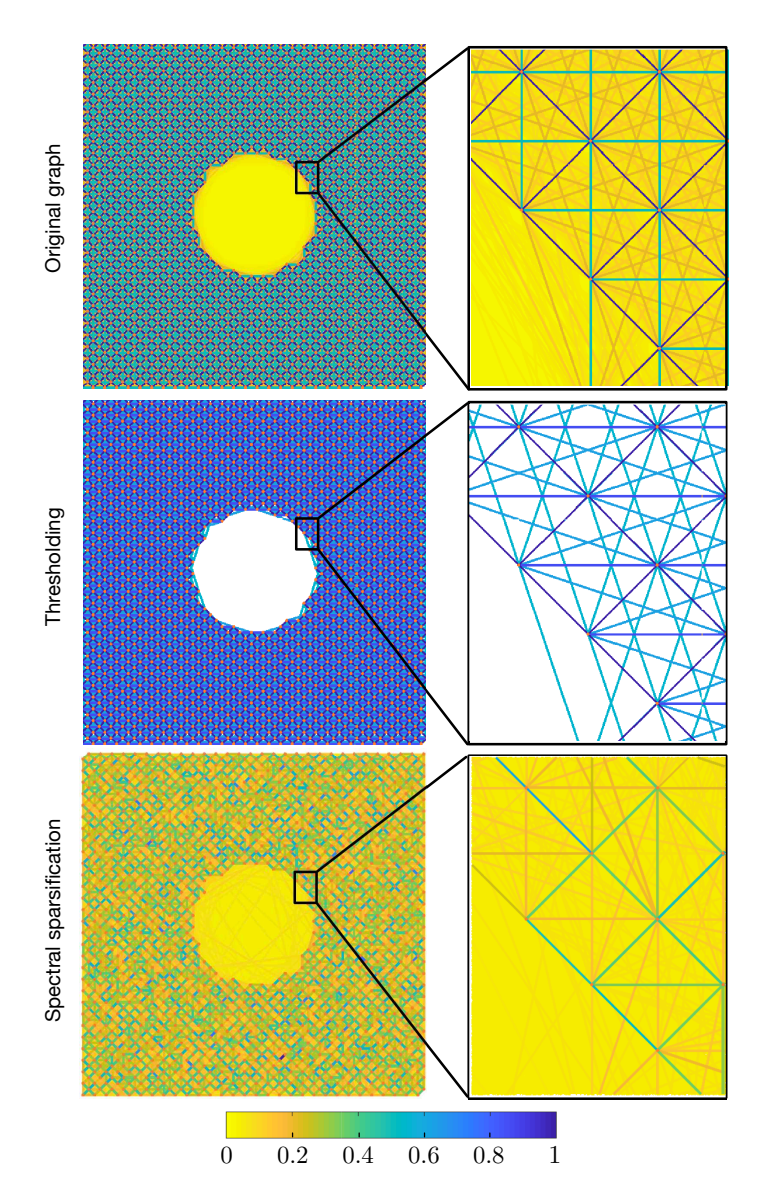


**FIGURE 3**. COULOMB FORCE GRAPHS WITH SPARSIFICATION BY THRESHOLDING AND SPECTRAL SPARSIFICATION. THE COLOR IS THE NORMALIZED EDGE WEIGHT.

The average normalized error is defined as

$$\frac{1}{N \left\| A_{ij} \right\|} \left\| \sum_{i} A_{ij}^{s} - \sum_{i} A_{ij} \right\|, \tag{14}$$

where  $||\cdot||$  represents the Euclidean norm and N is the number of nodes in the graph.

In Figure 6, we see that both spectral sparsification and thresholding have a low and comparable error, for the Lennard–Jones potential.

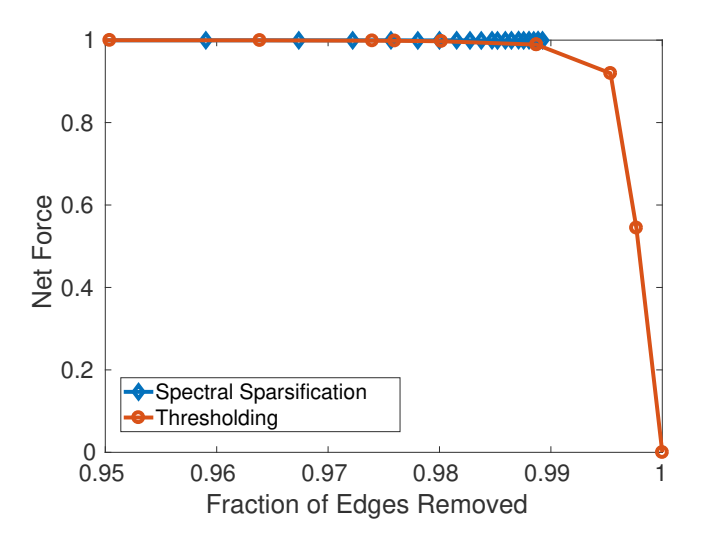


**FIGURE 4.**  $\sum_i \sum_j |F_{ij}|$  FOR LENNARD JONES POTENTIAL FOR BOTH SPECTRAL SPARSIFICATION AS A FUNCTION OF THE FRACTION OF EDGES REMOVED.

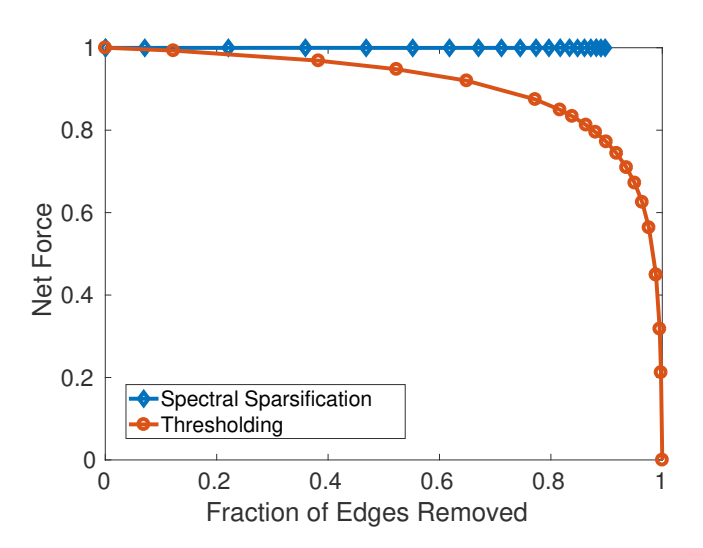


**FIGURE 5**.  $\sum_i \sum_j |F_{ij}|$  FOR COULOMB POTENTIAL FOR BOTH SPECTRAL SPARSIFICATION AS A FUNCTION OF THE FRACTION OF EDGES REMOVED.

However, for the Coulomb potential, the error in the spectral sparsification is significantly lower than for thresholding with similar fractions of edges removed, as shown in Figure 7. This suggests spectral sparsification has the ability improve simulations with long-range interactions.

It is important to note that sparsification maintains the mean degree distribution while maintaining a small error. In contrast, thresholding does not maintain degree distributions. An example of the changes in degree distribution is presented in Figure 8 for

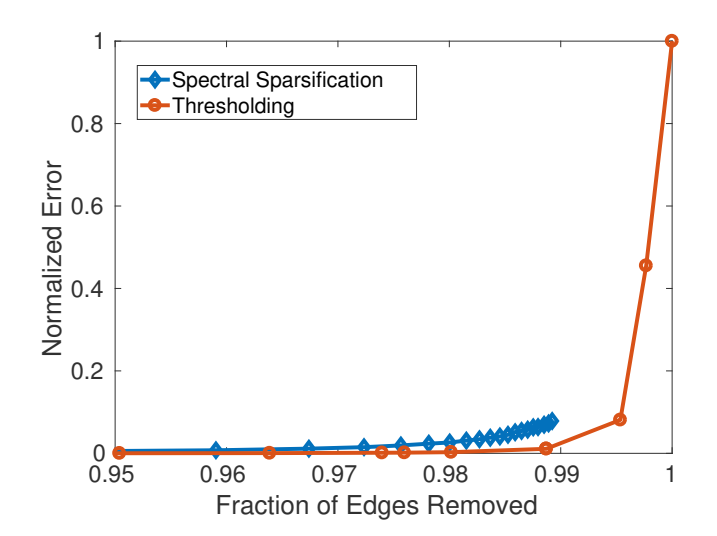


**FIGURE 6.** AVERAGE LOCAL NORMALIZED ERROR ESTIMATE FOR THE LENNARD–JONES POTENTIAL.

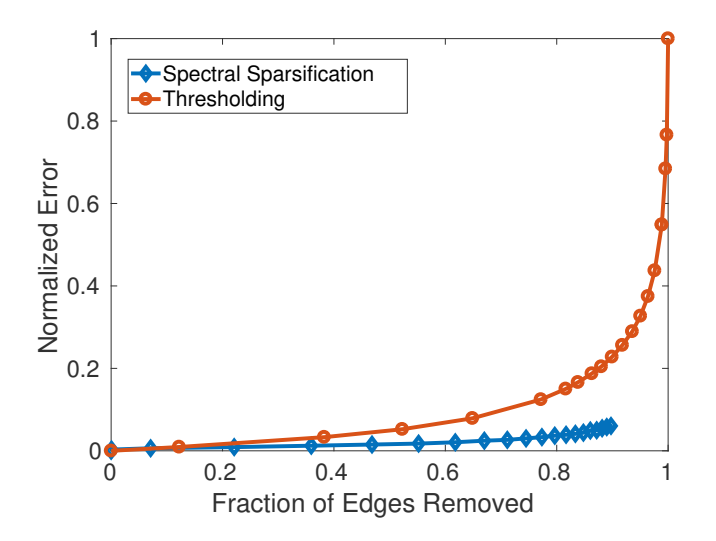


**FIGURE 7**. AVERAGE LOCAL NORMALIZED ERROR ESTIMATE FOR THE COULOMB POTENTIAL.

the Lennard–Jones potential. Qualitatively, spectral sparsification keeps the average degree constant while varying the degree distribution. While the distribution contains randomness, the algorithm keeps the Laplacian eigenvalue spectra similar. Keeping the average degree distribution constant and retaining the Laplacian spectra means spectral sparsification better approximates the forces in comparison to thresholding.

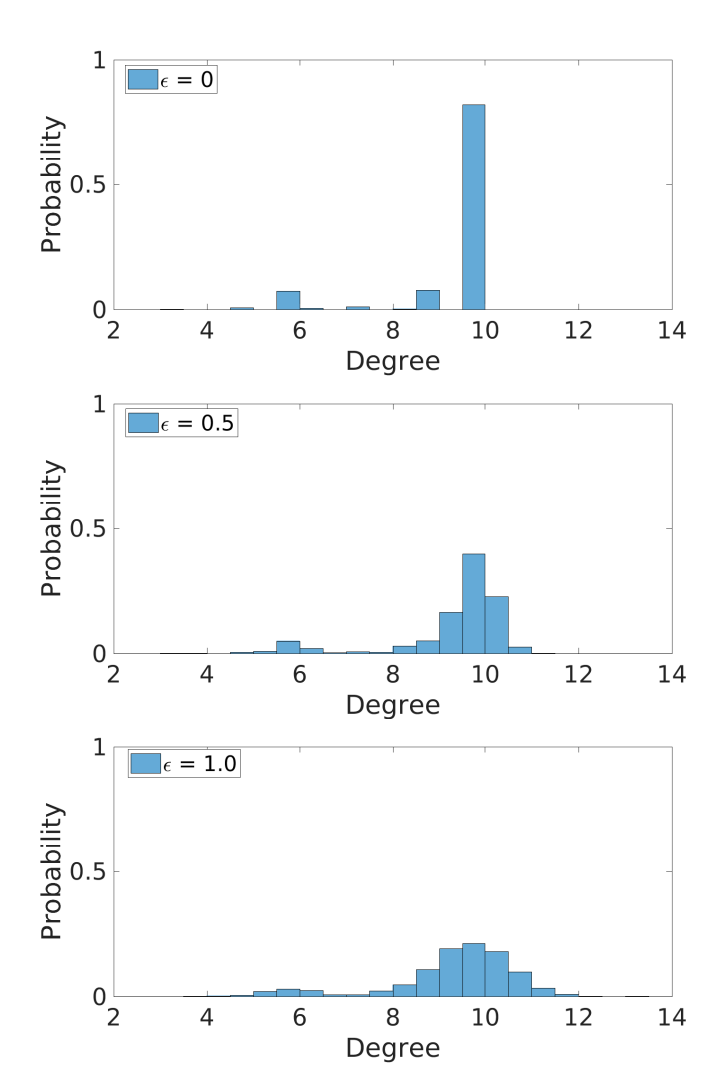


FIGURE 8. NORMALIZED DEGREE DISTRIBUTION FOR VARIOUS SPARSIFICATION LEVELS. THE DEGREE DISTRIBUTION REPRESENTS THE SUM OF THE FORCE INTERACTION ON EACH ATOM. THE PROBABILITY IS THE NUMBER OF ATOMS WITH DEGREE IN WITHIN RANGE DIVIDED BY THE TOTAL NUMBER OF ATOMS.

#### **Conclusions**

We have shown that spectral sparsification can provide a sparse representation of a material network while providing good approximations of the interatomic forces. In particular, we have shown that spectral sparsification produces lower error than thresholding for long-range electrostatic forces based on our two dimensional example problem. Importantly, sparsification maintains a conserved net force. This is significant because it suggests that sparsification is likely to have a lower error for macroscopic properties relative to thresholding. However, it does not necessarily keep the force on individual particles constant. It remains

to be seen if this significantly affects MD simulations.

Moving from the graph of the magnitude of forces to the kinematics and implementation into molecular dynamics simulations remains a task to be addressed in future work. It should be noted that there are a number of situations which should investigated. The work presented here dealt with a spherically symmetric potential on a two–dimensional plane. Sparsification might show improved results in anisotropic potentials (e.g. dipole-dipole interactions). Apart from dealing with anisotropic effects, the material studied here is crystalline. Spectral sparsification will likely be useful for random fields. Additionally, this work has not dealt with amorphous solids with defects. This is another area where spectral sparsification might perform well to approximate heterogeneous media on a network.

While full discussion of the computational costs and speed is beyond the scope of this paper, we give some preliminary estimates for comparison. For long-range forces, there are a number of different methods for summing long-range forces which range in computational costs of  $\mathcal{O}(n)$  to  $\mathcal{O}(n^2)$  [26–30]. Thresholding has a cost of  $\mathcal{O}(n)$  [1]. The presented sparsification algorithm is limited by calculation of the Moore-Penrose inverse which has a cost of  $\mathcal{O}(mn^2)$ , but otherwise has a cost of  $\mathcal{O}(n\log n)$  However, a discussion of parallel implementation as well as how the algorithm fits within the molecular dynamics simulations, e.g. number of edges cut and teh frequency of the algorithm, should be addressed.

In summary, the preliminary results are promising for approximating long–range atomistic forces in atomistic simulations with spectral sparsification. Such long–range forces are pervasive in multifunctional materials that exhibit strong polarization and magnetization effects including ferroelectric and ferromagnetic materials. There is also a host of other graph theoretic metrics not considered here which may be extracted from the edge distributions of our networks [13]. Such measures may provide further insight into structure-property relations and dynamic evolution in complex, multifunctional media.

#### **ACKNOWLEDGMENT**

The authors acknowledge the National Science Foundation for support of the work under EAGER grant #1648618. We also thank Prof. Shangchao Lin for productive discussions on molecular dynamics simulations.

# Appendix A: Graph Resistance

Effective graph resistance is proposed as generalization from networks of resistors (total resistance) of a graph [21]. The effective resistance between two nodes is similar to the effective resistance between two nodes in a circuit calculated by Ohm's law  $V = IR_{\rm eff}$ . In the case of networks of resistors, the weight of each edge is equivalent to the conductance  $w_{ij} = 1/R_{ij}$ . When

calculating the effective resistance, the current is always taken to be I=1, so the effective resistance  $\hat{R}_{ij}$  is then the potential difference across the network when unit current is put in at node i and unit current is removed at node j. The entire network resistance is simply the sum of the individual effective resistances  $R = \sum_{ij} \hat{R}_{ij}/2$ .

#### **REFERENCES**

- [1] Plimpton, S., 1995. "Fast parallel algorithms for short-range molecular dynamics". *Journal of Computational Physics*, 117.
- [2] Rapaport, D. C., 1995. *The Art of Molecular Dynamics Simulations*. Cambridge University Press.
- [3] Kong, L. T., 2011. "Phonon dispersion measured directly from molecular dynamics simulations". *Computer Physics Communications*, **182**(10), pp. 2201–2207.
- [4] Wunderlich, W., and Awaji, H., 2001. "Molecular dynamics simulations of the fracture toughness of sapphire". *Materials & Design*, 22(1), pp. 53 59.
- [5] Maruyama, S., 2000. "Molecular dynamics method for microscale heat transfer". *Advances in numerical heat transfer*, 2(6), pp. 189–226.
- [6] Wang, M., and Lin, S., 2015. "Ballistic thermal transport in carbyne and cumulene with micron-scale spectral acoustic phonon mean free path". *Scientific reports*, 5, p. 18122.
- [7] Wang, M., and Lin, S., 2016. "Anisotropic and ultralow phonon thermal transport in organic–inorganic hybrid perovskites: atomistic insights into solar cell thermal management and thermoelectric energy conversion efficiency". Advanced Functional Materials, 26(29), pp. 5297–5306.
- [8] Klein, M. L., and Shinoda, W., 2008. "Large-scale molecular dynamics simulations of self-assembling systems". *Science*, *321*(5890), pp. 798–800.
- [9] Davis, J. E., Ozsoy, A., Patel, S., and Taufer, M., 2009. "Towards large-scale molecular dynamics simulations on graphics processors". In Proceedings of the 1st International Conference on Bioinformatics and Computational Biology, BICoB '09, Springer-Verlag, pp. 176–186.
- [10] Shaw, D., 2010. "Using special-purpose hardware to achieve a hundred-fold speedup in molecular dynamics simulations of proteins". In 2010 IEEE International Symposium on Performance Analysis of Systems Software (IS-PASS), pp. 121–121.
- [11] Brown, W. M., Wang, P., Plimpton, S. J., and Tharrington, A. N., 2011. "Implementing molecular dynamics on hybrid high performance computers short range forces". *Computer Physics Communications*, **182**(4), pp. 898 911.
- [12] Brown, W. M., Kohlmeyer, A., Plimpton, S. J., and Tharrington, A. N., 2012. "Implementing molecular dynamics on hybrid high performance computers—particle—

- particle particle-mesh". Computer Physics Communications, 183(3), pp. 449–459.
- [13] Newman, M., 2010. Networks: An Introduction. Oxford University Press.
- [14] Nair, A. G., and Taira, K., 2015. "Network-theoretic approach to sparsified discrete vortex dynamics". *Journal of Fluid Mechanics*, **768**, pp. 549–571.
- [15] Taira, K., Nair, A. G., and Brunton, S. L., 2016. "Network structure of two-dimensional decaying isotropic turbulence". *Journal of Fluid Mechanics*, 795.
- [16] Nair, A. G., Taira, K., and Brunton, S. L., 2017. "Oscillator network based control of unsteady fluid flows". In 20th World Congress of the International Federation of Automatic Control. IFAC, Toulouse, July.
- [17] Singh, J., Vishwanath, R. B., Chaudhuri, S., and Sujith, R. I., 2017. "Network structure of turbulent premixed flames". *Chaos*, *27*, p. 043107.
- [18] Napp, N. E., and Adams, R. P., 2013. "Message passing inference with chemical reaction networks". In *Advances in Neural Information Processing Systems* 26, C. J. C. Burges, L. Bottou, M. Welling, Z. Ghahramani, and K. Q. Weinberger, eds. Curran Associates, Inc., pp. 2247–2255.
- [19] Papadopoulos, L., Puckett, J. G., Daniels, K. E., and Bassett, D. S., 2016. "Evolution of network architecture in a granular material under compression". *Physical Review E*, *94*(3), p. 032908.
- [20] Bassett, D. S., Owens, E. T., Porter, M. A., Manning, M. L., and Daniels, K. E., 2015. "Extraction of force-chain network architecture in granular materials using community detection". *Soft Matter, 11*(14), pp. 2731–2744.
- [21] Spielman, D. A., and Srivastava, N., 2011. "Graph sparsification by effective resistances". *SIAM Journal on Computing*, **40**(6), pp. 1913–1926.
- [22] Batson, J., Spielman, D. A., Srivastava, N., and Teng, S.-H., 2013. "Spectral sparsification of graphs: theory and algorithms". *Communications of the ACM*, *56*(8), pp. 87–94.
- [23] Griffiths, D., 1999. Introduction to Electrodynamics. Prentice Hall.
- [24] Benczúr, A. A., and Karger, D. R., 1996. "Approximating s-t minimum cuts in Õ(n2) time". In Proceedings of the Twenty-eighth Annual ACM Symposium on Theory of Computing, STOC '96, ACM, pp. 47–55.
- [25] Peleg, D., and Ullman, J. D., 1989. "An optimal synchronizer for the hypercube". *SIAM Journal on computing*, 18(4), pp. 740–747.
- [26] Rokhlin, V., 1985. "Rapid solution of integral equations of classical potential theory". *Journal of computational physics*, **60**(2), pp. 187–207.
- [27] Toukmaji, A., Sagui, C., Board, J., and Darden, T., 2000. "Efficient particle-mesh ewald based approach to fixed and induced dipolar interactions". *The Journal of Chemical*

- Physics, 113(24), pp. 10913-10927.
- [28] Hardy, D. J., Stone, J. E., and Schulten, K., 2009. "Multilevel summation of electrostatic potentials using graphics processing units". *Parallel Comput.*, 35(3), Mar., pp. 164–177.
- [29] Isele-Holder, R. E., Mitchell, W., and Ismail, A. E., 2012. "Development and application of a particle-particle particle-mesh ewald method for dispersion interactions". *The Journal of Chemical Physics*, 137(17), p. 174107.
- [30] Isele-Holder, R. E., Mitchell, W., Hammond, J. R., Kohlmeyer, A., and Ismail, A. E., 2013. "Reconsidering dispersion potentials: Reduced cutoffs in mesh-based ewald solvers can be faster than truncation". *Journal of Chemical Theory and Computation*, 9(12), pp. 5412–5420. PMID: 26592279.